RC23366 (W0410-053) October 8, 2004
Materials Science

IBM Research Report

Study of Spalling Behavior of Intermetallic Compounds during the Reaction between Electroless Ni-P Metallization and Lead-free Solders

Yoon-Chul Sohn, Jin Yu
KAIST
373-1, Guseong-Dong
Yuseong-Gu, Daejeon 305-701
Korea

Sung K. Kang, Da-Yuan Shih
IBM Research Division
Thomas J. Watson Research Center
P.O. Box 218
Yorktown Heights, NY 10598

Taek-Yeong Lee
Hanbat National University
San 16-1, DukMyoung-Dong
Yuseong-Gu, Daejeon
Korea

Research Division
Almaden - Austin - Beijing - Haifa - India - T. J. Watson - Tokyo - Zurich

Study of Spalling Behavior of Intermetallic Compounds During the Reaction Between Electroless Ni-P Metallization and Lead-free Solders

Yoon-Chul Sohn, Jin Yu, Sung K. Kang*, Da-Yuan Shih* and Taek-Yeong Lee**
Dept. of Mater. Sci. Eng., KAIST, 373-1, Guseong-Dong, Yuseong-Gu, Daejeon 305-701, Korea
*IBM T. J. Watson Research Center, 1101 Kitchawan Rd., Rt. 134, Yorktown Heights, NY 10598, USA
**Dept. of Mater. Eng., Hanbat National University, San 16-1, DukMyoung-Dong, Yuseong-Gu, Daejeon, Korea
sonyc@kaist.ac.kr, Tel. 82-42-869-4274, Fax. 82-42-869-8840

Abstract

Electroless Ni-P has been widely used for under bump metallization (UBM) of flip chip and surface finish layer in microelectronics packaging because of its excellent solderability, corrosion resistance, uniformity, selective deposition without photolithography, and also good diffusion barrier. However, the brittle fracture of solder joints and the spalling of intermetallic compound (IMC) associated with electroless Ni-P are critical issues for its successful applications. The mechanisms of the brittle fracture have been extensively investigated, but not fully understood yet. On the contrary, the spalling phenomenon has not been studied in detail, though IMC spalling could weaken the interfacial adhesion and also cause dewetting of flip chip solder bumps.

In this study, IMC spalling from an electroless Ni-P film was investigated with lead-free solders in terms of solder deposition methods (electroplating vs solder paste), P content in Ni-P layer (4.6, 9, and 13 wt.% P), and solder thickness (120 vs. 200μm). The reaction of Ni-P with Sn3.5Ag paste easily led to IMC spalling after 2 min reflow at 250°C while IMCs adhered to the Ni-P layer after 10 min reflow for the reaction with electroplated Sn or Sn3.5Ag. It has shown that both solder composition and deposition method are important for IMC spalling from a Ni-P layer. The spalling increased with P content in a Ni-P layer as well as with solder volume. Ni_3Sn_4 intermetallics formed as a needle-shaped morphology in the early stage and changed into a chunky shape. Needle-shaped compounds exhibited a higher propensity for spalling from aNi-P layer than chunky shaped compounds because molten solder can easily penetrate into the interface between needle-shaped IMCs and the P-rich layer. A reaction between the penetrated Sn and the P-rich layer formed a NiSnP layer. The poor adhesion between the Ni_3Sn_4 compound and the NiSnP layer caused the IMC spalling. Dewetting of solder from the NiSnP layer, however, didn't occur even after spalling of most IMCs. The wetting reactions of Pb-free solders on electroless Ni-P layers are also discussed.

Introduction

Solder bumps in flip chip technologies of microelectronic devices is an interconnection for electrical data and thermal energy dissipation from an IC chip to a substrate.[1] The substrate in microelectronics packaging is usually organic PCB (Print Circuit Board), or LTCC (Low Temperature Cofired Ceramic).[2,3] The solder joint between an IC chip and a substrate is a key interconnection for the electrical performance and reliability of an electronic system.

A reliable solder joint can be formed by a metallurgical reaction between a molten solder and UBM on a chip or metallization on a substrate, which produces stable IMCs at the joint interfaces.[4,5] Pb-containing solders have been extensively used in microelectronic interconnections. Recently, the industry is searching for Pb-free solders to replace Pb-containing solders for environmental reasons as well as consumers' desire for green products. Most of Pb-free solders are Sn-based alloys such as Sn-3.5Ag, Sn-3.8Ag-0.7Cu, Sn-0.7Cu and others (all in wt.% if specified otherwise). The interfacial reactions between Pb-free solders and UBM have become a critical issue, because both the Sn content in the solders and their reflow temperatures are higher than the conventional Pb-Sn eutectic solder.[6-12] The previous studies on the interfacial reactions between high-Sn solders and thin film UBM showed the IMC spalling. The IMC spalling is a reliability concern because it can result in dewetting of molten solder during joining and thereby yielding weak adhesion of solder joints during field operation.[13,14]

The spalling of Cu-Sn IMC from a chip was found during the reaction between eutectic SnPb solder and Cu-based UBM such as Ti/Cu, Cr/Cu/Au and phased-in Cr-Cu/Cu/Au.[15-17] In the case of Ti/Cu and Cr/Cu/Au UBM, the solder consumed all Cu film and then IMCs were separated from the interface [15,16] because the IMCs did not wet the adhesion layer such as Cr or Ti layer. The phased-in Cr-Cu UBM also failed in preventing the spalling of Cu_6Sn_5 formed in eutectic SnPb while it prevented the spalling of Cu_3Sn in 95Pb5Sn solder.[17] A tensile and shear testing with Cr/Cu metallization and SnPb eutectic solder showed that the fracture strength decreased with annealing time due to IMC spalling from the Cr layer.[13] The spalling of Ni_3Sn_4 from Ni-based UBM (Ti/Ni) was also observed, eventually led to the dewetting of the molten solder from the Ti surface.[14] The thin film metallization of Al/Ni(V)/Cu, however, was reported to form stable Cu_6Sn_5 adhesion to Ni(V) without spalling during the reaction with eutectic SnPb.[18]

Reactions between Pb-free solders and Al/Ni(V)/Cu UBM showed different behaviors from the reactions with eutectic SnPb. In Sn-3.5Ag-1.0Cu, the Ni(V) layer was gradually dissolved into the molten solder during multiple reflows and the spalling of $(Cu,Ni)_6Sn_5$ IMC was observed.[7] In addition, the Ni metallizaton on the substrate side was reported to enhance dissolution of the interfacial IMC formed adjacent to the Ni(V) layer at the chip side.[8]

Recently, electroless Ni-P metallization has received great attention because of its low cost and the simple processing steps. The interfacial reactions between Pb-free solders and electroless Ni-P have been investigated.[9,10] The interfacial IMCs in the Sn-rich solders containing Cu such as Sn-0.7Cu and Sn-3.8Ag-0.7Cu had good adhesion with Ni-P while Sn-3.5Ag and Sn-2Ag-2Bi alloys formed needle-shaped IMCs that spalled off from the Ni-P.[9] IMC spalling from the Ni-P layer appears to be quite different from other metallizations. IMCs on Ni-P spall off before consuming all the Ni-P layer, while IMCs on other metallizations usually spall off after consuming all the reaction layer. The previous studies on the reactions between Pb-free solders and Ni-P, however, had considered only the effect of solder composition. In this study, we have systematically investigated the IMC spalling from Ni-P in Sn-rich, Pb-free solders in terms of solder deposition method, P content in Ni-P and reflow time.

Experimental procedure

Cu foil (25μm thick) and sputtered Cr/ Cu (30nm/4μm) on Si wafer were used as substrates, which was cleaned with acetone and treated in a 0.5M H_2SO_4 solution to remove surface oxides. The Cu layer was then activated with a Pd solution before electroless Ni-P plating. Electroless Ni-P films were deposited for three different P content (4.6, 9 and 13 wt.% P) with Technic EN 1400, EN 9185 and EN 3600 solutions (from Technic Inc, Cranston, RI), respectively. Thicknesses of Ni-P film were 9μm on Cu foil and 5μm on Si/Cr/Cu substrate, respectively.

The P content in a Ni-P layer was analyzed by an electron probe microanalyzer (EPMA). The microstructure of Ni-P is expected to vary depending on P content; nanocrystalline for 4.6 wt.% P, amorphous with some crystallites for 9 wt.% P, and completely amorphous for 13 wt.% P.[19-23]

Pure Sn and eutectic Sn-3.5Ag were used as solder materials in the present study. A Sn layer (120 and 200μm thickness) was deposited on a Ni-P layer by electroplating with Solderon SC solution (from Shipley company, Marlborough, MA) with a current density of 37.5 mA/cm^2. 120μm thick Sn-3.5Ag layer was also deposited on a Ni-P layer by electroplating using UTB TS-140 solution (from Unicon Ishihara company, Japan) with 24 mA/cm^2. Sn-3.5Ag paste (from Heraeus Ltd.) was applied on a Ni-P layer through a solder mask having an opening of 10mm diameter and 120 μm thickness. Sn3.5Ag preform of 130μm thickness was also used for comparison. And then, samples were reflowed for 0.5 to 30min in a N_2 atmosphere to investigate IMC spalling and interfacial reactions between the Ni-P metallization and Pb-free solders. Water-soluble flux (WS613 from Alpha Metals) was applied onto Sn3.5Ag preform before reflow, while electroplated solders were reflowed without flux.

Cross-sectional scanning electron microscopy (SEM) and transmission electron microscopy (TEM) with energy dispersive x-ray spectroscopy (EDX) were used for microstructure and composition analysis. TEM samples were prepared by a standard procedure with dicing, mechanical thinning, dimpling and ion milling. The electron microscopy was carried out using JEOL JEM-3010 electron microscope operated at 300kV. To prepare a cross-sectional SEM specimen, the reflowed samples were mounted with epoxy and then cross-sectioned metallographically. The samples were then etched with 3%HCl-5%HNO_3-92%CH_3OH (in vol.%) solution for several minutes to reveal their microstructures. In the present study, the Ni-P films are denoted as Ni-4.6P, Ni-9P and Ni-13P specimens after their P weight percent in the films.

Results

A. Effect of solder deposition method on IMC spalling

Fig. 1. shows cross-sectional views of Ni-9P film reacted with Sn3.5Ag paste (120μm thick), electroplated Sn3.5Ag (120μm thick), and Sn3.5Ag preform (130μm thick) after 10min reflow at 250°C. Most of Ni_3Sn_4 IMC formed in solder paste spalled off the Ni-9P surface as shown in Fig. 1(a), while the Ni-Sn IMC formed at the interface of electroplated Sn3.5Ag/Ni-9P adhered well to the Ni-P layer as shown in Fig. 1(b). Ni_3Sn_4 IMC formed in Sn3.5Ag preform partially spalled off 10~20% of the Ni-P surface in Fig. 1(c). In electroplated Sn3.5Ag, Ni_3Sn_4 spalling was observed after about 30min reflow. Therefore, spalling rate of Ni_3Sn_4 compounds was much slower in electroplated solder than solder paste.

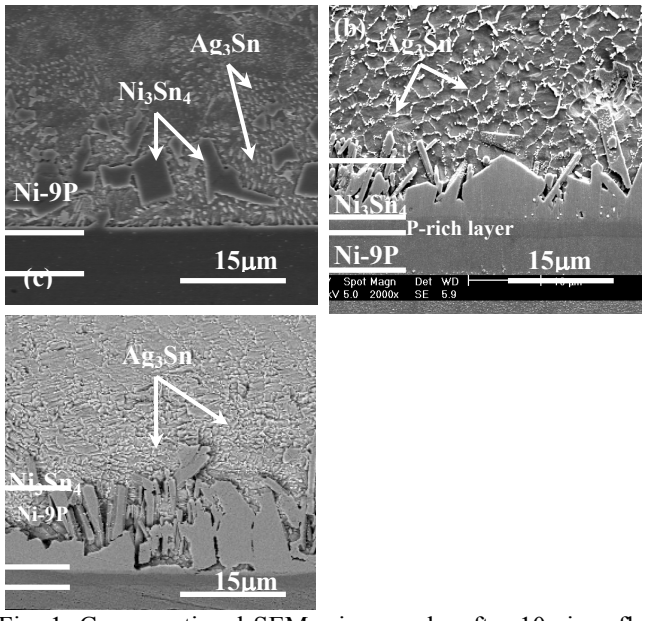

Fig. 1. Cross-sectional SEM micrographs after 10min reflow at 250°C.
(a) 9μm thick Ni-9P/120μm thick Sn3.5Ag paste
(b) 9μm thick Ni-9P/120μm thick electroplated Sn3.5Ag
(c) 5μm thick Ni-9P/130μm thick Sn3.5Ag preform

The different spalling behaviors between electroplated and paste solder can be understood by noting the different conditions at the interfaces. For an electroplated solder, before reflow, there would be chemical bonding between solder and the Ni-P metallization, but not for solder paste. In addition, since a solder paste is a mixture of metal powder

and flux, the Ni-P surface would be in contact with the flux at early stage of reflow. For the case of electroplated solder, no flux exists at the interface.

B. Effect of P content on IMC spalling

Fig. 2 shows the interfacial reactions as a function of P content (Ni-4.6P, Ni-9P and Ni-13P), reaction time (1 and 10 min) and solder deposition methods (Sn3.5Ag solder paste, electroplated Sn and Sn3.5Ag preform). In case of Sn3.5Ag paste, for a short reaction of 1 min at 250°C, Ni_3Sn_4 IMCs still adhered on the Ni-4.6P layer in Fig. 2(a), but most IMCs spalled off the Ni-13P surface as shown in Fig. 2(c). This indicates IMC spalling increases with the P content in the Ni-P layer. Meanwhile, for the electroplated Sn, IMCs adhered well on all of the Ni-P films even after 10 min reflow at 250°C as shown in Fig. 2(d), (e), and (f). Spalling behaviors in Sn3.5Ag preform showed the same trend with those in Sn3.5Ag paste as shown in Fig. 2(g), (h), and (i). Table I summarizes the spalling behaviors of Ni_3Sn_4 IMC on the Ni-P layer in terms of solder deposition method, P content, and reaction time.

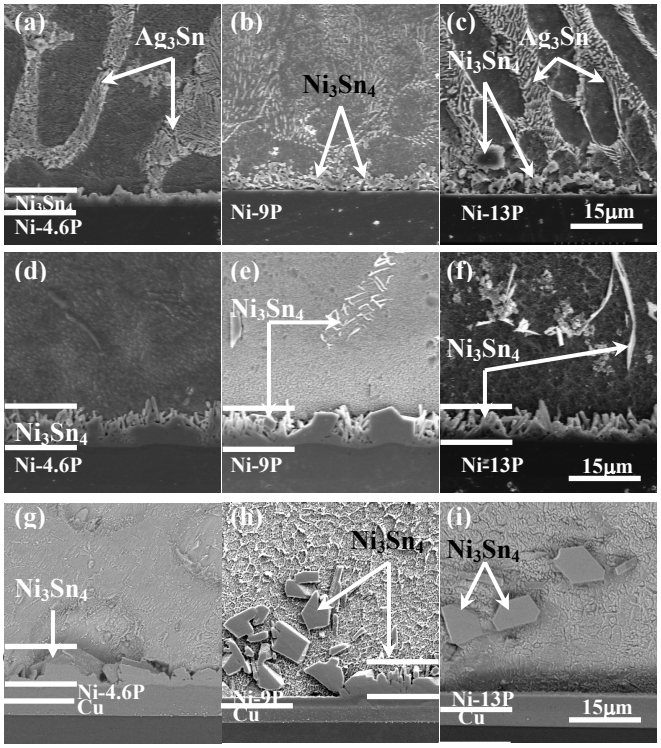

Fig. 2. Cross-sectional SEM micrographs of (a) Ni-4.6P, (b) Ni-9P and (c) Ni-13P (9μm) reacted with Sn3.5Ag paste (120μm) at 250°C, 1 min, (d) Ni-4.6P, (e) Ni-9P and (f) Ni-13P (9μm) reacted with electroplated Sn (120μm) at 250C, 10 min, and (g) Ni-4.6P, (h) Ni-9P and (i) Ni-13P (5μm) reacted with Sn3.5Ag preform (130μm) at 250°C, 10 min, (all pictures in same magnification.)

In addition to P content, IMC spalling is dependent on reflow time. For Sn3.5Ag paste samples, IMC spalling was not much observed after 1 min reflow at 250°C in Fig. 2(a) and (b), but severely occurred after 10 min reflow in Fig. 1(a). In case of Sn3.5Ag preform, IMC spalling was more dependent on P content than reaction time. For example, the spalling area didn't much increase with reaction time in case of Ni-9P. For electroplated Sn and Sn3.5Ag samples, IMC spalling was not detected even after 10 min reflow.

C. Effect of solder volume on IMC spalling

Fig. 3(a), (b) and (c) show cross-sectional SEM micrographs of 9 μm thick Ni-9P films reacted with the electroplated Sn of two different thicknesses; 120 and 200 μm. The morphology of Ni-Sn IMCs and the spalling behaviors were affected by the solder volume on the Ni-P layer. With 120 μm thick solder, IMC spalling was not observed even after 10 min reflow as shown in Fig. 2(e), while IMC spalling occurred in 200 μm thick solder after 10 min reflow as shown in Fig. 3(c). In addition, IMC morphology changed from the needle-shape into a chunk-shape in 120 μm thick solder after 10 min reflow, while this morphological change did not occur in 200 μm thick solder.

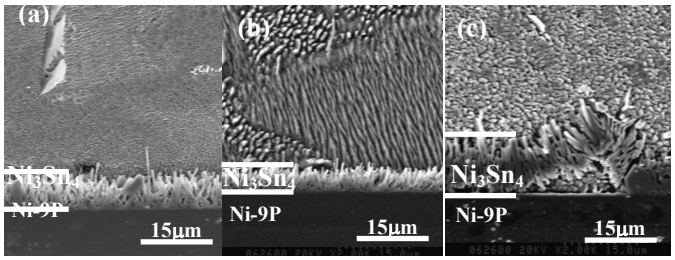

Fig. 3. Cross-sectional SEM micrographs of (a) 9μm thick Ni-9P layer reacted with 120μm thick electroplated Sn after 2min reflow, (b) 9μm thick Ni-9P layer reacted with 200μm thick electroplated Sn after 2min reflow and (c) after 10 min reflow at 250°C.

Discussion

A. Crystallization-assisted spalling of Ni_3Sn_4 compounds

Fig. 4(a) shows cross-sectional views of Ni-9P film reacted with 130μm thick Sn3.5Ag preform after 10min reflow at 250°C. Ni_3Sn_4 compounds formed on the Ni-9P film and partially spalled off the surface. Note that structure of the Ni-P layer in the left-hand side (IMCs spalled) is different from that in the right-hand side (IMCs adhered). Magnified views of IMC spalled area and well-adhered area are presented in Fig. 4(b) and (c), respectively. In IMC adhered area, dark P-rich layer was found between Ni_3Sn_4 compounds and unreacted Ni-P film. P content of the P-rich layer and unreacted Ni-P layer was measured to be about 25 at.% and 16 at.% (9 wt.%) respectively, as shown in Fig. 4(b). It shows Ni_3P phase formed in the P-rich layer [24-26], while the composition of unreacted amorphous Ni-P film remained same as that of as-plated Ni-9P film. On the other hand, in IMC spalled area, a NiSnP layer formed on the Ni-P layer with 33 at.% P as shown in Fig 4(c). A thickness of the Ni-P film in IMC spalled area was measured to be 1.7μm, which is much smaller than 3μm in IMC adhered area. Spalling of

Ni_3Sn_4 IMCs accelerated crystallization of amorphous Ni-P film as shown in Fig. 4(b) and (c). After 10min reaction, without IMC spalling, the half of unreacted amorphous Ni-9P film remained, while the Ni-9P film totally crystallized after spalling.

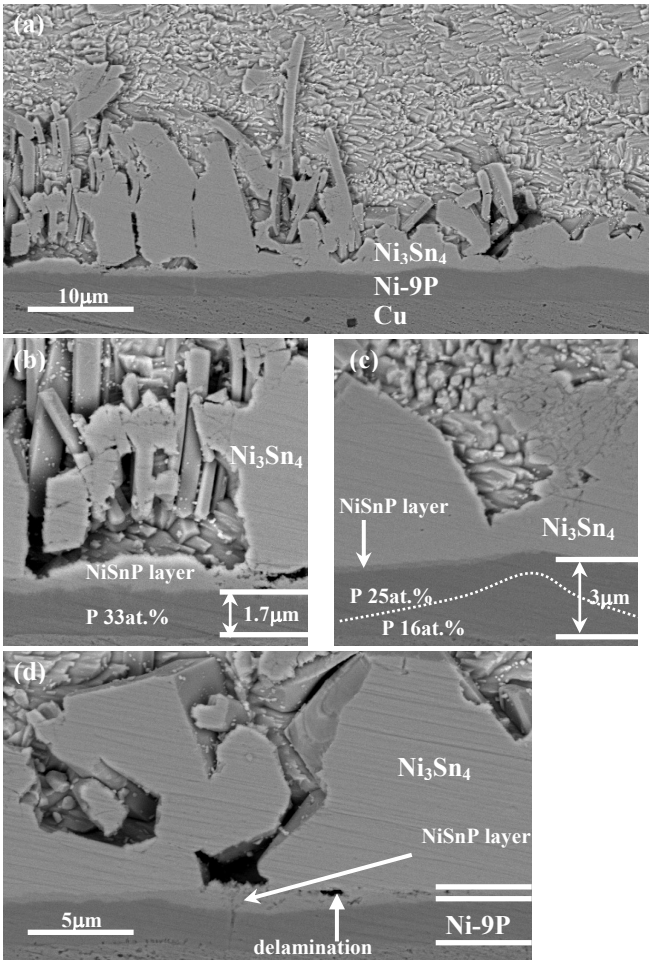

Fig. 4. Cross-sectional SEM micrographs of (a) 5μm thick Ni-9P layer reacted with 130μm thick Sn3.5Ag preform after 10min reflow, (b) magnified view of lefthand side of (a), (c) magnified view of righthand side of (a) and (d) 5μm thick Ni-9P layer reacted with 130μm thick Sn3.5Ag preform after 30min reflow at 250°C.

A formation of nanocrystalline NiSnP layer between Ni_3Sn_4 and Ni_3P layer has been reported.[27,28] However, the role of this layer on IMC spalling has not been reported. In the present study, a reaction between Sn penetrated under Ni_3Sn_4 IMCs and crystalline Ni_3P layer (P-rich layer) was found to form the NiSnP layer. It was confirmed by reacting Sn3.5Ag preform with crystallized Ni-P (Ni_3P+Ni) film heated up to 480°C.[30] IMC spalling occurred at the interface of Ni_3Sn_4/NiSnP. Fig. 4(d) shows an initiation of Ni_3Sn_4 compound spalling from the NiSnP layer. Therefore, supression of the NiSnP layer growth would prevent IMC spalling.

Sn penetration to the interface between IMCs and Ni-P layer would be easier through needle-shaped IMCs, which have many channels for molten Sn than through chunky IMCs. Since reactions of Cu-containing solders with the Ni-P films are known not to form needle-shaped IMCs [9], it is understood why solders such as Sn-0.7Cu and Sn-3.8Ag-0.7Cu are more resistant to IMC spalling from the Ni-P metallization.

Cross-sectional TEM was conducted to identify the microstructure and phase of the Ni-9P film reacted with Sn3.5Ag. After IMC spalling, the Ni-9P film transformed into Ni_3SnP/Ni_2P after 30min reaction with Sn3.5Ag as shown in Fig. 5. The Ni_3SnP layer consisted of 20~100nm grains and the Ni_2P layer had large columnar grains. Since the Ni_3P phase first formed as a crystalline layer underneath the IMC before spalling, it is expected that Ni_2P was transformed from Ni_3P, not from the as-plated Ni-P. A formation of the Ni_3SnP/Ni_2P layer was confirmed by reactions between Sn3.5Ag and the Ni-13P film.[29] And a thin NiSnP layer underneath Ni_3Sn_4 compound which didn't spall was also identified as Ni_3SnP phase in recent publication.[28]

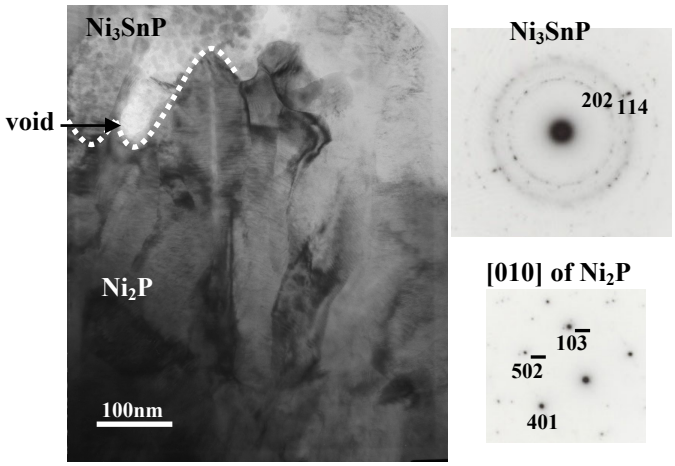

Fig. 5. Cross-sectional TEM image of 5μm thick Ni-9P layer after 30min reaction with 130μm thick Sn3.5Ag preform at 250°C.

B. Spalling of needle-shaped IMCs

The interfacial IMCs (Ni_3Sn_4) initially formed as a needle-shaped morphology as shown in Fig. 3(a) and (b). And they agglomerated into a chunky shape during the growth as shown in Fig. 2(d), (e) and (g). But Ni-Sn IMCs in some samples spalled off before they changed into a chunky morphology. The needle-shaped IMCs showed higher propensity for spalling than the chunky ones, which was also shown in Fig. 4(a) and (b).

For simplicity, assuming the IMC shape as a hexagonal column, the interfacial area between Ni_3Sn_4 and P-rich layer can be roughly estimated for needle-shaped vs chunk-shaped compound by measuring the width of each IMC. As an example, the width of a needle is measured to be about 0.7μm in Fig. 3(a) and that of a chunky IMC is about 9μm in Fig. 2(e). The area ratio of a chunky IMC to a needle-type IMC is about 165. Therefore, a large chunky IMC in Fig. 2(e) can replace more than 100 needle-like IMCs, even if some channels are considered among the IMCs. As reported in the study of the wetting reaction of molten solder on Cu [30], the

channels among IMCs provide paths for molten solder to reach interface of Ni_3Sn_4/P-rich layer and finally to detach IMCs from the NiSnP layer formed on the P-rich layer.

The change of needle-like IMCs into chunky ones is thermodynamically favorable since the large interfacial area between Ni_3Sn_4 needles and molten solder can be reduced. Kinetically, molten Sn diffuses fast through the channels among the IMCs, even found inside the Ni_3P layer.[27] Therefore, during the reaction, IMC coarsening and diffusion of molten Sn to form the NiSnP layer compete each other. If IMC coarsening is faster, the channels among the IMCs reduce and the NiSnP layer formation and IMC spalling slow down. If Sn diffusion through the channels is faster, IMCs spall off the NiSnP surface formed on the P-rich layer. IMC spalling will occur after molten solder penetrates the interface between Ni_3Sn_4 and the P-rich layer, forming two interfaces; Ni_3Sn_4/NiSnP and NiSnP/the P-rich layer. The penetration length should be 10 times longer for the chunky IMC in Fig. 2(e) than the needle-like IMC in Fig. 3(a). However, during the IMC coarsening, the channel area for the supply of molten solder will dramatically decrease, by more than 100 times. Consequently, IMC spalling would take longer time.

C. Sn penetration through Ni-P

If Sn penetrates into the Ni-P layer and reaches to a Cu underlayer, it can react with Cu to form intermetallic compounds.[12] Therefore, the thickness and reactivity of the Ni-P layer are important. Sn penetration was found after 30 min reflow through 5μm thick Ni-4.6P and Ni-13P films, while not found in Ni-9P films. Fig. 6(a) and (b) show cross-sectional views of Ni-4.6P films reacted with 130μm thick Sn3.5Ag preform after 10min and 30min reflow at 250°C, respectively. In case of the reactions of Ni-4.6P/Sn3.5Ag, thin P-rich layer (Ni_3P) formed underneath the Ni_3Sn_4 IMCs and the interface between Ni_3Sn_4 and the Ni-4.6P films was very rough as shown in Fig. 6(a) and (b). During 30min reflow, some areas in 5μm Ni-4.6P layer were all consumed and Sn penetrated through the channels in Ni-P layer and then reacted with Cu to form $(Cu,Ni)_6Sn_5$ IMC. If the Cu layer was not thick enough, a weak interface would form between $(Cu,Ni)_6Sn_5$ compound and the substrate as shown in Fig. 6(b).

In case of of the reactions of Ni-13P/Sn3.5Ag, after 0.5min reflow, most IMCs spalled off the NiSnP surface and the Ni_3SnP layer grew with reflow time. Ni_3SnP thickness was linearly dependent on square root of reaction time($t^{1/2}$), which meant diffusion controlled growth. A diffusion coefficient for Ni_3SnP growth was determined to be about 4.1×10^{-12} cm^2/s using the relation $x^2=Dt$. This value is about 4 times lower than the diffusion coefficient for Ni_3P growth in Ni-P/67Sn-37Pb system.[24] The Ni-13P films crystallized fast due to fast IMC spalling as was the case with spalled area of Ni-9P sample in Fig. 4(b). After 10min reflow, some cracks formed vertically through the crystallized Ni-13P layer, but not filled up with Sn yet. These cracks were getting larger and eventually filled with Sn with increasing reaction time. However, until 30min reflow, Sn didn't react with the Cu underlayer in this case. The cracks seem to form due to volume contraction induced tensile stress that was generated during the fast crystallization of the Ni-13P film. Therefore, a Ni-P film with low P content would not be good because of irregular consumption of the film, while a Ni-P film with high P content would not be useful due to severe IMC spalling and the brittle crystalline layer formed with some cracks inside.

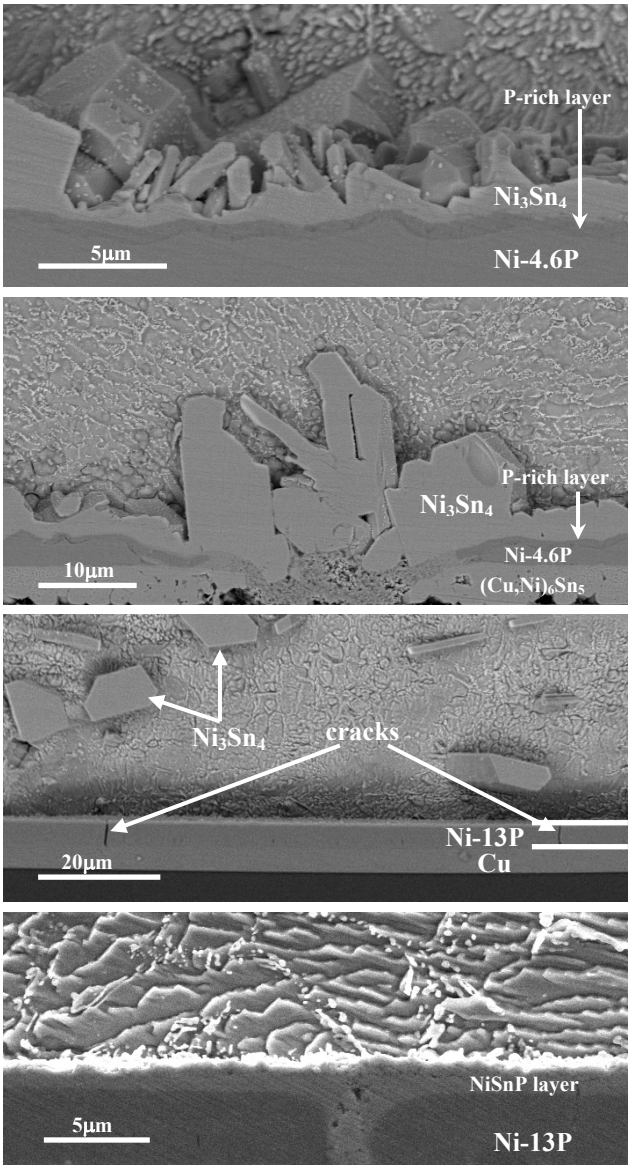

Fig. 6. Cross-sectional SEM micrographs of (a) 5μm thick Ni-4.6P layer reacted with 130μm thick Sn3.5Ag preform after 10min reflow, (b) after 30min reflow and (c) 5μm thick Ni-13P layer reacted with 130μm thick Sn3.5Ag preform after 10min reflow, (d) after 30min reflow at 250°C.

Conclusions

IMC spalling during the wetting reaction of Sn and Sn3.5Ag on electroless Ni-P metallization was investigated in terms of P content in Ni-P, deposition method, and reaction time. From this study, the following conclusions are drawn:

1) The propensity for IMC spalling from a Ni-P surface generally increases with increasing P content and reaction time.

2) The solder deposition method is important to determine the IMC spalling behavior; the solder deposited from solder paste has a higher tendency of IMC spalling than electrodeposited solders under an equivalent reflow condition.

3) The morphology of Ni-Sn IMCs is found to influence their spalling behavior; a needle-like morphology is more prone to spall in comparison with a chunky morphology. The fast spalling of needle-like IMCs is explained by a reaction kinetic factor such as channels among the needle-like IMCs.

4) IMC spalling from a Ni-P layer is closely related with the crystallization process. The reaction between Sn and crystalline Ni_3P forms a NiSnP layer. Spalling occurs at the interface of Ni_3Sn_4/NiSnP. The crystallization of unreacted amorphous Ni-P film is accelerated after IMC spalling.

5) Sn penetration through Ni-P is found in 5μm thick Ni-4.6P and Ni-13P layer after 30min reflow. It is explained by irregular consumption of the Ni-4.6P layer and by fast crystallization and crack formation in the Ni-13P layer.

Acknowledgments

This work was conducted under the KAIST-IBM joint study program and supported by the Center for Electronic Packaging Materials (CEPM) of Korea Science and Engineering Foundation.

References

1. Rao R. Tummala, Eugene J. Rymaszewski and Alan G. Klopfenstein, Microelectronics Packaging Handbook (2nd ed.), Chapman & Hall (1997), Part2, Ch8.
2. M. Baker-Pole. "Printed circuits-Origin and Development, Part2", *Circuit World* vol.10, No.3 (1984), pp. 8.
3. Y. Shimade, K. Utsumi, M. Suzuki, H. Takamizowa, M. Nitta and T. Watari. "low firing temperature multiplayer glass-ceramic substrate" *IEEE Trans-CHMT* vol.6, No.4 (1983), pp. 382.
4. S. K. Kang and V. Ramachandran, "Growth Kinetics of Intermetallic Phases at the Liquid Sn and Solid Ni Interface" *Scripta Met.* Vol.14, No.4 (1980), pp. 421.
5. G. A. Walker and P. W. Dehaven and C. C. Goldsmith, *Proc 34th Electronic Components and Technology Conf*, 1984, pp. 125.
6. S. K. Kang, R. S. Rai and S. Purushothaman, "Interfacial Reactions During Soldering with LEAD-Tin Eutectic and Lead (Pb)-Free, Tin-Rich Solders" *J. Electron. Mater.* Vol.25, No.7 (1996), pp. 1113.
7. M. Li, F. Zhang, W. T. Chen, K. Zeng, K. N. Tu, H. Balkan and P. Elenius, "Interfacial microstructure evolution between eutectic SnAgCu solder and Al/Ni(V)/Cu thin films" *J. Mater. Res.* Vol.17, No. 7 (2002), pp. 1612.
8. F. Zhang, M. Li, C. C. Chum and K. N. Tu, "Influence of substrate metallization on diffusion and reaction at the under-bump metallization/solder interface in flip-chip packages" *J. Mater. Res.* Vol. 17, No. 11 (2002), pp. 2757.
9. J. W. Jang, D. R. Frear, T. Y. Lee and K. N. Tu, "Morphology of interfacial reaction between lead-free solders and electroless Ni-P under bump metallization" *J. Appl. Phys.* Vol. 88, No. 11 (2000), pp. 6359.
10. S. K. Kang, D. Y. Shih, K. Fogel, P. Lauro, M. J. Yim, G. Advocate, M. Griffin, C. Goldsmith, D. W. Henderson, T. Gosselin, D. King, J. Konrad, A. Sarkhel and K. J. Puttlitz, "Interfacial Reaction Studies on Lead (Pb)-Free Solder Alloys" *Proc 51th Electronic Components and Technology Conf*, 2001, pp. 448.
11. G. Ghosh, "Dissolution and Interfacial Reactions of Thin-film Ti/Ni/Ag Metallizations in Solder Joints" *Acta mater.* Vol. 49 (2001), pp. 2609-2924.
12. M. O. Alam, Y. C. Chan and K. N. Tu, "Effect of reaction time and P content on mechanical strength of the interface formed between eutectic Sn-Ag solder and Au/electroless Ni(P)/Cu bond pad" *J. Appl. Phys.* Vol. 94, No. 6 (2003), pp. 4108.
13. C. Y. Liu, Chih Chen, A. K. Mal and K. N. Tu, "Direct correlation between mechanical failiure and metallurgical reaction in flip chip solder joints" *J. Appl. Phys.* Vol. 85, No. 7 (1999), pp. 3882.
14. P. G. Kim, J. W. Jang, T. Y. Lee and K. N. Tu, "Interfacial reaction and wetting behavior in eutectic SnPb solder on Ni/Ti thin films and Ni foils" *J. Appl. Phys.* Vol. 86, No. 12 (1999), pp. 6746.
15. H. K. Kim, K. N. Tu and P. A. Totta, "Ripening-assisted asymmetric spalling of Cu-Sn compound sheroids in solder joints on Si wafers" *Appl. Phys. Lett.* Vol. 68, No. 16 (1996) pp. 2204.
16. Ann A. Liu, H. K. Kim, K. N. Tu and P. A. Totta, "Spalling of Cu_6Sn_5 spheroids in the soldering reaction of eutectic SnPb on Cr/Cu/Au thin films" *J. Appl. Phys.* Vol. 80, No. 5 (1996), pp. 2774.
17. G. Z. Pan, Ann A. Liu, H. K. Kim, K. N. Tu and P. A. Totta, "Microstructure of phased-in Cr-Cu/Cu/Au bump-limiting metallization and its soldering behavior with high Pb content and eutectic PbSn solders" *Appl. Phys. Lett.* Vol. 71, No. 20 (1997), pp. 2946.
18. C. Y. Liu, K. N. Tu, T. T. Sheng, C. H. Tung, D. R. Frear and P. Elenius, "Electron microscopy study of interfacial reaction between eutectic SnPb and Cu/Ni(V)/Al thin film metallization" *J. Appl. Phys.* Vol. 87, No. 2 (2000), pp. 750.
19. Kreye, H., Müller, F., Lang, K., Isheim, D. and Hentschel, T., *Z. Metallkd.* Vol. 86 (1995), pp. 184.
20. Kreye, H., Müller, H.-H. and Petzel, T., *Galvanotechnik* Vol. 77 (1986), pp. 561.
21. Dietz, G. and Schneider, H. D., *J. Phys.: Condens. Matter* Vol. 2 (1990), pp. 2169.
22. S. H. Park and D. N. Lee, "A study on the microstructure and phase transformation of electroless nickel deposits" *J. Mater. Sci.* Vol. 23 (1988), pp. 1643.
23. K. H. Hur, J. H. Jeong and D. N. Lee, "Microstructure and crystallization of electroless Ni-P deposits" *J. Mater. Sci.* Vol. 25 (1990), pp. 2573.

24. J. W. Jang, P. G. Kim, K. N. Tu, D. R. Frear and P. Thompson, "Solder reaction-assisted crystallization of electroless Ni-P under bump metallization in low cost flip chip technology" *J. Appl. Phys.* Vol. 85, No. 12 (1999), pp. 8456.
25. Y. C. Sohn, Jin Yu, S. K. Kang, W. K. Choi and D. Y. Shih, "Study of the reaction mechanism between electroless Ni-P and Sn and its effect on the crystallization of Ni-P" *J. Mater. Res.* Vol 18, No. 1 (2003), pp. 4-7.
26. Y. C. Sohn, Jin Yu, S. K. Kang, W. K. Choi and D. Y. Shih, "Effect of Phosphorus Content on the Reaction of Electroless Ni-P with Sn and Crystallization of Ni-P" *J. Electron. Mater.*, accepted for publication.
27. K. Zeng, K. N. Tu, "Six cases of reliability study of Pb-free solder joints in electronic packaging technology" *Mater. Sci. and Eng R* Vol. 38 (2002), pp.55-105.
28. C. W. Hwang, K. Suganuma, M. Kiso and S. Hashimoto, "Interface microstructures between Ni-P alloy plating and Sn-Ag-(Cu) lead-free solders" *J. Mater. Res.* Vol. 18, No. 11 (2003), pp. 2540.
29. Y. C. Sohn, Jin Yu and T. Y. Lee, unpublished work.
30. K. N. Tu and K. Zeng, "Tin-lead (SnPb) solder reaction in flip chip technology" *Mater. Sci. and Eng R* vol. 34 (2001), pp. 1-58.

Table I. Morphologies and spalling behaviors of Ni_3Sn_4 intermetallic compounds

P content in Ni-P	solder	deposition method	thickness (μm)	reflow (min)	IMC morphologies	spalling
4.6 wt.%	Sn3.5Ag	paste	120	1	needle	none
				2	N. D.	partially
				10	N. D.	mostly
		preform	130	0.5	needle	none
				10	chunk>needle	none
				30	chunk>needle	none
	Sn	plating	120	1	needle	none
				2	needle>chunk	none
				10	chunk>needle	none
9 wt.%	Sn3.5Ag	paste	120	1	needle	partially
				2	N. D.	mostly
				10	N. D.	mostly
		preform	130	0.5	needle	partially
				10	chunk>needle	partially
				30	chunk>needle	partially
		plating	120	2	needle>chunk	none
				10	chunk>needle	none
	Sn	plating	120	1	needle	none
				2	needle>chunk	none
				10	chunk>needle	none
13 wt.%	Sn3.5Ag	paste	120	1	N. D.	mostly
				2	N. D.	mostly
				10	N. D.	mostly
		preform	130	0.5	N. D.	mostly
				10	N. D.	mostly
				30	N. D.	mostly
				2	needle	none

	Sn	plating	120	10	needle	none

N. D. : not determined